A Sparsified Vector Potential Equivalent Circuit Model for Massively Coupled Interconnects

Hao Yu, Lei He

Abstract— *The vector potential equivalent circuit (VPEC) model was introduced for accurately modeling inductive interconnects, and the main computation complexity is inverting the full inductance matrix. In this paper, we develop two sparse approximated inversions to extract the sparsified VPEC model without full inductance matrix inversion. One is a heuristic windowing, and the other is the Schur's windowing based on the generalized Schur's interpolation algorithm. Both methods have faster extraction time and higher accuracy compared to the existing truncation-based sparsification, and the Schur's windowing achieves the best accuracy. Furthermore, the resultant windowed VPEC circuits can be directly simulated in SPICE with orders of magnitude speedup and less than* 3% *error compared to the full PEEC model.*

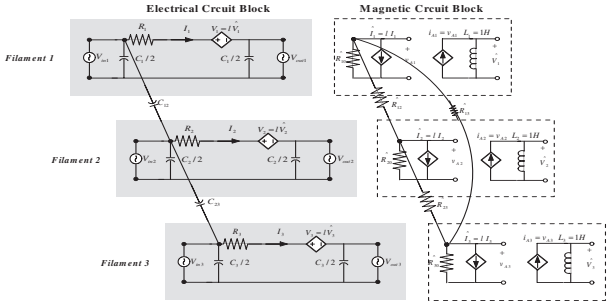

Fig. 1. The Vector Potential Equivalent Circuit model for three filaments.

I. Introduction

As VLSI technology advances with increased operating speed, inductive effects of on-chip interconnects become increasingly significant in terms of delay and signal integrity. Because the loop-inductance model needs to specify the return path of a current and therefore difficult to use, the growing portion of interconnects is modeled by the Partial Element Equivalent Circuit (PEEC) model [1], where each wire forms virtual loop with infinity. The accurate PEEC model requires detailed discretization of interconnects, and the full PEEC circuit may have an extremely high complexity because of coupling inductances between any pair of interconnect segments. For example, for 128-bit bus with 20 segments per line, it will result 3,278,080 elements with 162M storage of SPICE netlist. Consequently it makes the direct SPICE analysis formidable. Because the partial inductance matrix in PEEC is not diagonal dominant, simply truncating off-diagonal elements leads to negative eigenvalues such that the truncated inductance matrix loses passivity [2]. Several inductance sparsification methods have been proposed with guaranteed passivity by studying the inverse of inductance matrix [3]–[5], but the resulting circuit models can not be simulated by SPICE. Using *effective resistances* to model inductive interconnects [6], a vector potential equivalent circuit (VPEC) is derived by inverting the full inductance matrix [7]. The VPEC model can be analyzed by SPICE, and direct truncation (off-diagonal elements) based sparsifications is developed with guaranteed passivity.

However the full matrix inversion used in [7] is not efficient for large scale interconnects. Furthermore, simply truncating small off-diagonal entries of the inversed matrix may not be accurate enough. In this paper, we introduce two windowing techniques that avoid the inversion of full inductance matrix and obtain better extraction efficiency and accuracy than the sparsification method in [7]. We first review the VPEC model in Section II, and then present a heuristic windowing method in Section III and a rigorous Schur's windowing method based on the generalized Schur's interpolation in Section IV. We compare various VPEC models in in Section V, and conclude the paper in Section VI.

II. Full Vector Potential Equivalent Circuit

Same as in FastHenry [8] with the magneto-quasi-static assumption, the conductor can be divided into a number of rectilinear *filaments*. The current density is *constant* over the cross-section of the filament. In this paper, we use superscripts x, y, z to denote spatial components of a vector variable. Let $\mathbf{A}$ be the *vector potential*, which is determined by the distribution of the current density J. Then J^k and A^k are the components in k-direction ($k = x, y, z$). We further use the subscript i for variables associated with filament a_i, and every filament a_i has a length l by adequately discretizations in the k-direction. To model the inductive effect, we start with differential Maxwell equations in terms of $\mathbf{A}$ [9]:

$$\nabla^2 A^k = -\mu J^k \tag{1}$$

$$\frac{\partial A^k}{\partial t} = -E^k \tag{2}$$

where the vector potential $\mathbf{A}$ is in the z-direction same as the current density $\mathbf{J}$, $\mathbf{E}$ is the electrical field, and μ is the permeability constant. Note that the resistive voltage drop by $(-\nabla^k \phi)$ is not included in (2) since we are interested in the inductive voltage drop here. Given the distribution of the current density J^k, the vector potential A^k is determined by

$$A^k = \frac{\mu}{4\pi} \int \frac{J^k}{|\mathbf{r} - \mathbf{r}'_i|} d\tau(\mathbf{r}'_i) \tag{3}$$

For filament a_i, when (1) is integrated within the volume τ_i of filament a_i, using *Gauss' Law*: we can obtain

$$\begin{aligned} -\mu \int_{\tau_i} J^k d\tau &= \int_{S_i} \nabla A^k \cdot d\mathbf{S} \\ &= \mathcal{B}^k_{i0} + \sum_{j \neq i} \mathcal{B}^k_{ij} \end{aligned} \tag{4}$$

Note that the surface integral $\int_{S_i} d\mathbf{S} \cdot \nabla A^k$ is actually the *magnetic flux* caused by the filament current of a_i in τ_i. It is consisted of following parts: (i) the flux to the infinity (vector potential ground) $\mathcal{B}^k_{i0}$; and (ii) the flux to all other filaments a_j ($j \in N, j \neq i$) $\mathcal{B}^k_{ij}$. However, to explicitly determine the value of $\mathcal{B}^k_{ij}$ is difficult because it is hard to estimate the partition of the flux between filament a_i, all other filament a_j, and the vector potential ground.

By defining the *filament vector potential* [6] as the *average* volume integral of A^k within τ_i:

$$A^k_i = \frac{1}{\tau_i} \int_{\tau_i} A^k(\mathbf{r}) d\tau(\mathbf{r}) \tag{5}$$

We can define an effective coupling resistance

$$\hat{R}^k_{ij} = -\mu \frac{(A^k_i - A^k_j)}{\mathcal{B}^k_{ij}} \tag{6}$$

to model (i.e., replace) the mutual inductive coupling between a_i

This paper is partially supported by NSF CAREER award CCR-0401682, SRC grant 1100, a UC MICRO grant sponsored by Analog Devices, Fujitsu Laboratories of America, Intel and LSI Logic, and a Faculty Partner Award by IBM. Address comments to lhe@ee.ucla.edu.

H. Yu and L. He are with the Electrical Engineering Department, University of California Los Angeles, CA 90095 USA. email:{hy255,lhe}@ee.ucla.edu.

and a_j. In addition, there also exists an effective ground resistance to model the self inductive effect:

$$\hat{R}^k_{i0} = -\mu \frac{A^k_i}{\mathcal{B}^k_{i0}} \tag{7}$$

To extract the effective resistance $\hat{R}^k_{ij}$ and $\hat{R}^k_{i0}$, the integration-based approach in [6] needs determine the localized flux $\mathcal{B}^k_{ij}$ ($j \in n_i$), where n_i is the set of adjacent filaments to a_i. As we discussed above, the explicitly calculation of $\mathcal{B}^k_{ij}$ is hard, and only considering the localized flux will further lose the accuracy. In fact, the integration-based VPEC model needs optimize the "controlled-volume" for each filament. It becomes computation inefficient when the system size is large. To solve this problem , a full inversion based extraction is proposed in [7] based on the non-local KCL equation:

$$\frac{A^k_i}{\hat{R}^k_{i0}} + \sum_{j \neq i} \frac{(A^k_i - A^k_j)}{\hat{R}^k_{ij}} = lI^k_i \tag{8}$$

where the summation in (8) is not localized ($j \in N, j \neq i$). The physical meaning of the effective resistance is: *Given a unit current change at ith filament, the vector potential observed at jth filament is exactly $\hat{R}^k_{ij}$ when all other filaments are connected to vector potential ground.* As shown in [7], the effective resistances can be efficiently extracted below:

$$\hat{R}^k_{ij} = -\frac{1}{l^2 K^k_{ij}}, \qquad \hat{R}^k_{i0} = \frac{1}{l^2 K^k_{ii} + \sum_{j \neq i} l^2 K^k_{ij}} \tag{9}$$

where $K^k = (L^k)^{-1}$.

We present a SPICE compatible VPEC model for three filaments in Fig.1. The model is consisted of two blocks: the electrical circuit (PEEC resistance and capacitance) and the magnetic circuit (VPEC effective resistance and unit inductance). They are connected by the controlled sources. It includes following components: (1) The resistance R_i and capacitance C_i in the electrical circuit are the same as those in the PEEC model; (2) A dummy voltage source to sense current I^k_i in the electrical circuit controls $\hat{I}^k_i$ in the magnetic circuit; (3) A voltage controlled current source is used to relate $\hat{V}^k_i$ and $\hat{I}^k_i$ with gain $g = 1$ in the magnetic circuit; (4) A voltage source V^k_i in the electrical circuit is controlled by $\hat{V}^k_i$ in the magnetic circuit; (5) Effective resistances including ground $\hat{R}^k_{i0}$ and coupling $\hat{R}^k_{ij}$ are used to represent the strength of inductances in the magnetic circuit; and (6) A unit inductance L_i in the magnetic circuit is used to: (i) take into account the time derivative of A^k_i; and (ii) preserve the magnetic energy from the electronic circuit.

Although the full inversion based extraction can help us obtain the correct/accurate effective resistance, recall our purpose is to sparsify the massively coupled inductive effect. In [7], the sparsification of VPEC model is by truncating off-diagonal elements from the effective resistance matrix as it has the property of strictly diagonal dominance. However, it needs the initial full inversion and this full inversion becomes inefficient when circuit size is large. In the following sections, we solve this problem by obtaining a *sparse approximated inverse* of the inductance matrix to build a sparsified VPEC model. The first one is based on heuristic windowing, which is fast to attack large sized circuit. The second is based on Schur's windowing, which is sparsely interpolated from the original matrix with the *maximum entropy*, i.e., the sparse approximation with the best accuracy.

III. Heuristic Windowing

As discussed below, we extended a heuristic windowing method in [4] to construct sparsified VPEC model, where the entry of the inverse matrix can be approximately reconstructed from the entry of sub-matrices in full matrix L, where each sub-matrix is corresponding to a coupling window of each wire when it acts as the active aggressor.

- Windowed Extraction: We first specify one aggressor m and all victims within a specified window of band b, and then construct a sub-matrix $L^{(m)}$ that:

$$L^{(m)}_{ij} = \begin{cases} L_{ij} & \text{if (i, j) inside the window;} \\ 0 & \text{if (i, j) outside the window.} \end{cases}$$

We can obtain a K-element vector $\mathbf{k}^{(m)}$ by: $L^{(m)}\mathbf{k}^{(m)} = \mathbf{i}^{(m)}$, where $\mathbf{i}^{(m)}$ is the unit current vector of mth aggressor: $\mathbf{i}^{(m)}_n = \delta_{mn}$. We then iterate above procedures for all conductors in turn as active aggressor. Because this process is only related to the sub-matrix, the complexity of full inversion is much reduced.

- Heuristic Matrix Construction: Next, we merge all $\mathbf{k}^{(m)}$ vectors into one complete, sparse matrix K' that approximates the inversion of full inductance matrix. The entry of K' is selected by:

$$K'_{mn} = K'_{nm} = max(\mathbf{k}^{(m)}_n, \mathbf{k}^{(n)}_m) \tag{10}$$

where $\mathbf{k}^{(m)}_n$ means the susceptance between nth victim inside the window of mth aggressor, and it is negative [5] with sufficient discretization. For a stable system, its circuit matrix needs to be symmetric positive definite (s.p.d). However, under step (a) the $\mathbf{k}^{(m)}_n$ is not necessary equal to $\mathbf{k}^{(n)}_m$ [4]. The heuristic in (10) guarantees that

$$K'_{mm} \geq \sum_n |K'_{mn}| \tag{11}$$

and preserves the symmetry, i.e., the resulting K' is s.p.d. Due to the heuristic nature of (10), we call this method as *heuristic windowing*. We finally construct VPEC model based on (9) with the approximated K' matrix. The resultant windowed VPEC model can be directly simulated in SPICE.

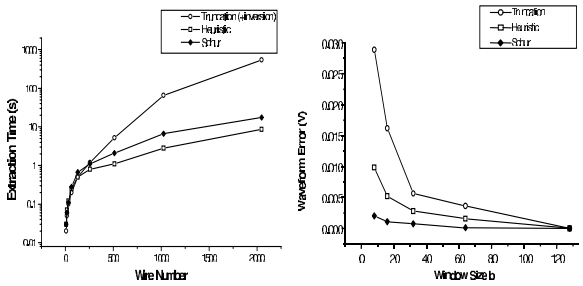

Fig. 2. The comparisons of extraction efficiency and accuracy of truncation, heuristic windowing,and Schur's windowing based sparsifications.

IV. Schur's Windowing

The Schur's windowing method is based on the generalized Schur's interpolation, a computation-efficient algorithm for the inverse of a symmetric positive definite matrix with a pre-specified band structure S [10]. It is briefly illustrated as follows. A staircase band structure S is first specified to a s.p.d matrix X. Then a hyperbolic rotation matrix θ is defined and utilized to interpolate a generation matrix M defined from X. Note that this interpolation is iterated within S, and it can automatically preserve the s.p.d property. After sequential interpolations we obtain a matrix X_{ME} that satisfies the *maximum entropy condition* [10], [11], and its inverse X^{-1}_{ME} has zeros in positions corresponding to the *complement* of the band S. The generalized Schur's interpolation was used for the sparse capacitance matrix extraction [11] and substrate conductance matrix extraction [12]. We apply this technique to generating the sparsified VPEC model and comparing its performance with aforementioned heuristic windowing in terms of efficiency and accuracy.

A. Preliminary

1) Admissible Matrix: For a given $N \times N$ s.p.d partial inductance matrix L, its diagonal matrix is $D = diag[L_{11}, L_{22}, ..., L_{NN}]$. The normalized inductance matrix is $\mathcal{L}^{(0)} = D^{-1/2} L D^{-1/2}$, and can be rewritten as

$$\mathcal{L}^{(0)} = U^{(0)} + V^{(0)\,T}, \qquad U^{(0)} = I + V^{(0)} \tag{12}$$

where ^{T} means the transpose operation, $V^{(0)}$ is a strictly upper triangular matrix, and I is a $N \times N$ unity matrix.

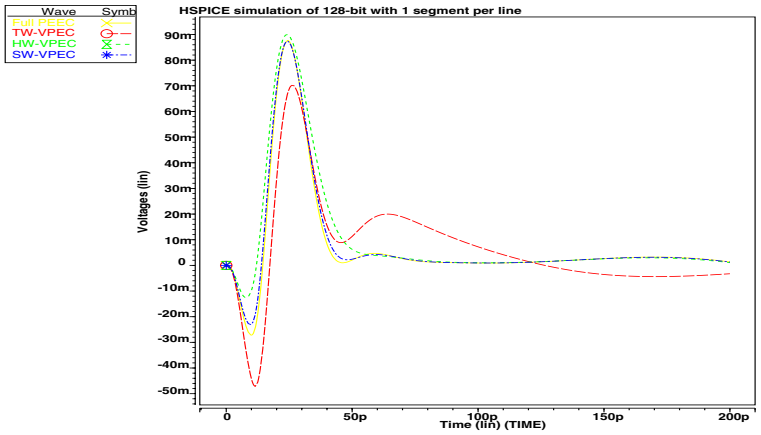

Fig. 3. Transient response at far-end of 2nd bit of 128-bit bus.

Using $U^{(0)}$ and $V^{(0)}$, a $N \times 2N$ *generation matrix* is defined as $M^{(0)} = [U^{(0)} \quad V^{(0)}]$. It can generate $\mathcal{L}^{(0)}$ by the following operation:

$$M^{(0)} J M^{(0)\,T} = U^{(0)} U^{(0)\,T} - V^{(0)} V^{(0)\,T} = \mathcal{L}^{(0)} \tag{13}$$

where a $2N \times 2N$ J-unitary matrix is:

$$J = \begin{bmatrix} I & 0 \\ 0 & -I \end{bmatrix}$$

Generally, $M = [U \quad V]$ is called *admissible* if its generated matrix $MJM^T = UU^T - VV^T$ is symmetric positive definite. For example, $M^{(0)}$ is admissible since $\mathcal{L}^{(0)}$ (inductance matrix) is symmetric positive definite.

2) Hyperbolic Rotation Matrix: We further define the hyperbolic rotation matrix θ. It is a $2N \times 2N$ unit matrix except following entries:

$$\theta_{i,i} = \theta_{j+N,j+N} = \frac{\rho_{ij}}{\sqrt{1-\rho^2}} \tag{14}$$

$$\theta_{i,j+N} = \theta_{j+N,i} = \frac{1}{\sqrt{1-\rho^2}} \tag{15}$$

where ρ is the *refection coefficient* to be specified. Note that the product of a sequential hyperbolic rotation matrices is still a hyperbolic rotation matrix. Further the following Lemma [11] is given:

Lemma 1: Any right-sided operation of an admissible matrix M with hyperbolic rotation matrix θ still results an admissible matrix: $M' = M\theta$ with $M' = [U' \quad V']$.

It means that the s.p.d property of the generated matrix $\mathcal{L}'$ $(M'JM')$ is preserved.

B. Generalized Schur's Interpolation

The interpolation basically utilizes a sequential hyperbolic rotation matrix to multiply with M matrix. During each iteration the θ matrix is updated by the transformed M matrix from last iteration. The iteration stops till exploring all the specified entries in the band S. The finalized hyperbolic rotation matrix Θ will then be used to calculate the approximated inverse. Note that the interpolation actually eliminate entries of V_{ij} in M matrix, where index (i,j) is in the specified band. We first illustrate how to eliminate one entry and then the entire band.

Given a hyperbolic rotation matrix θ_{ij} with refection coefficient:

$$\rho_{ij} = -\frac{V_{ij}}{U_{ii}} \tag{16}$$

one entry V_{ij} in M can be eliminated by:

$$M' = [U' \quad V'] = [U \quad V]\theta_{ij} \tag{17}$$

where V'_{ij} equals 0 in the transformed matrix M'.

Then we can explain how to eliminate the specified band S in $V^{(0)}$. Recall that $V^{(0)}$ is part of $M^{(0)}$ defined from $\mathcal{L}^{(0)}$. Assume a staircase band S is specified for matrix $\mathcal{L}^{(0)}$ with band width b $(1 \le b \le N)$. Based on the order of off-diagonal $[d_1, d_2, ..., d_b]$ in band S, the elimination begins at the first off-diagonal and ends at the bth off-diagonal. The corresponding sequential hyperbolic rotation matrix is

$$\Theta^{(b)} = \prod_{l=1,\ldots,b} \theta^l, \qquad \theta^l = \prod_{(i,j)\in d_1,\ldots,d_b} \theta^l_{ij} \tag{18}$$

where the reflection coefficient for θ^l during lth-iteration is updated by:

$$\rho^l_{ij} = -\frac{V^{l-1}_{ij}}{U^{l-1}_{ii}} \tag{19}$$

As shown in part C, matrix $\Theta^{(b)}$ is used to obtain the sparse approximated inverse $K^{(b)}$.

After bth iteration, the generation matrix is:

$$M^{(b)} = [U^{(b)} \quad V^{(b)}] = [U^{(0)} \quad V^{(0)}]\Theta^{(b)} \tag{20}$$

where all the entries of $V^{(b)}_{ij}$ with $(i,j) \in S$ in $M^{(b)}$ are eliminated. The generated inductance matrix $\mathcal{L}^{(b)}$ now becomes

$$M^{(b)} J M^{(b)\,T} = U^{(b)} U^{(b)\,T} - V^{(b)} V^{(b)\,T} \tag{21}$$

According to Lemma 1, $\mathcal{L}^{(b)}$ is a s.p.d matrix and hence it can be decomposed by a upper-triangular matrix $W^{(b)}$, i.e.,

$$\mathcal{L}^{(b)} = W^{(b)} W^{(b)\,T} \tag{22}$$

We further give following implicit relation between $U^{(b)}$, $V^{(b)}$, $W^{(b)}$ and $\Theta^{(b)}$ for proofs [11] of Theorem 1 in the next part.

$$\Theta^{(b)} = \begin{bmatrix} U^{(b)\,T} & -V^{(b)} \\ -V^{(b)\,T} & U^{(b)} \end{bmatrix} \begin{bmatrix} W^{(b)\,-T} & 0 \\ 0 & W^{(b)\,-1} \end{bmatrix}$$

C. Maximum Entropy Extension

The most intuitively question for the sparse approximated inversion problem is: *how to find the best approximated inverse X^{-1} that has as many as possible zero elements?* It has been shown in [10], [11] that such a matrix satisfies the following *maximum entropy condition*: **Given a s.p.d matrix X with the specified off-diagonal band S, there exits a unique s.p.d matrix X_{ME} that satisfies maximum entropy extension condition: (i) $(X_{ME})_{ij} = X_{ij}$ for $(i,j) \in S$; (ii) $(X^{-1}_{ME})_{ij} = 0$ for $(i,j) \notin S$.** It was proved in [11] that the

matrix obtained by generalized Schur's interpolation satisfies above conditions:

Lemma 2: The $X^{(l)}$ matrix generated by lth-order generalized Schur's interpolation satisfies maximum entropy condition. It is lth-order maximum entropy extension of original matrix X.

Consequently we have the following theorem:

Theorem 1: $\mathcal{L}^{(b)}$ is the bth-order maximum entropy extension of $\mathcal{L}^{(0)}$. It satisfies: $(\mathcal{L}^{(0)} - \mathcal{L}^{(b)})_{ij} = 0$ for all $(i, j) \in S^{(b)}$, and its inverse $\mathcal{K}^{(b)}$ has following properties:
(i) entries not in S is zero; (ii) $\mathcal{K}^{(b)}$ is s.p.d and is determined by: $W^{(b)^{-T}} W^{(b)^{-1}}$, where the upper-triangular $W^{(b)^{-1}}$ is calculated from:

$$[W^{(b)^{-T}} \quad W^{(b)^{-1}}] = [I \quad I]\Theta^{(b)}. \tag{23}$$

Recall that $\Theta^{(b)}$ is determined in the interpolation equation (18). The $\mathcal{K}^{(b)}$ matrix found above is therefore the *best sparse approximated inverse* of $\mathcal{L}^{(0)}$ to the bth-order. This has been also confirmed in the experiment. Finally we need denormalize the $\mathcal{K}^{(b)}$ into K' by: $K' = D^{1/2}\mathcal{K}^{(b)}D^{1/2}$. The sparsified VPEC model can be then obtained via K'.

When the specified structure is not a regular band structure, a permutation matrix P can be found such that a transformed matrix $X' = PXP^T$ to reconstruct a band. Compared to the heuristic windowing, this algorithm : (i) automatically guarantees the s.p.d property without additional heuristic selection as in [4]; (ii) is the maximum entropy extension to give the best accuracy to approximate of the original matrix. Moreover, its computation complexity is similar to the heuristic windowing, but the practical implementation in experiment shows the heuristic windowing is faster.

V. Experimental Results

We have implemented these two windowed VPEC methods in C code. We assume the copper ($\rho = 1.7 \times 10^{-8}\Omega \cdot m$) interconnect with low-$k$ ($\epsilon = 2$) dielectric. The partial inductance is extracted by FastHenry [8], where each wire segment is modeled by one filament, and coupling between any pair of segments (including segments in a same line) is considered. Note that when frequency is beyond 10GHz, the assumption needs modified by means of volume filaments decomposition to take into account the skin and proximity effects. The capacitance is extracted by FastCap [13]. Because the capacitive coupling is a short-range effect, only adjacent couplings are considered. Furthermore, interconnect driver and receiver are modeled by resistance $R_d = 100\Omega$ and loading capacitance $C_L = 2fF$. Below, we present results for aligned parallel bus lines. A 1-V transient voltage with 10ps rising time is applied to the first line, and all other lines are quiet. All circuits are simulated by HSPICE on SUN Ultra-5 workstation.

We present the efficiency of the extraction by truncation (+inversion), heuristic windowing (HW) and Schur's windowing (SW) in Fig. 2 (a), where wee extract the VPEC model by these three methods for wires up to 2000 bits. For similar model size, we use a geometrical window during truncation (TW). As shown in [7], TW method considers the effective coupling resistances only inside a truncating window (N_W, N_L), where N_W and N_L are the numbers of coupled segments in directions of bus width and length, respectively. Here the geometrical window size for truncation is (N_W, N_L) = (8, 1), and is b = 8 for both heuristic and Schur's windowing. The extraction time for truncation-based method includes the full inversion and truncation. Clearly, when the scale of interconnects is small (below 128-bit), the truncation-based method is actually as efficient as the two window-based methods. But when the scale of interconnects becomes larger, the window-based extraction is much faster than the truncation-based approach for the 2048-bit bus: with a 90X speedup (8.6s vs. 543.1s) by heuristic windowing, and a 27X speedup (20.5s vs. 543.1s) by Schur's windowing. Therefore, it is more efficient to apply the (heuristic) winnowed VPEC model for the large scale interconnects. In Fig. 2 (b), we further give the accuracy comparison for these three sparsifications with different window sizes (b=64, 32, 16, 8) for a 128-bit bus example. When reduced the window size, the reduced simulation time and memory, but also reduced accuracy are observed for all the sparsified models. However, since the Schur's interpolation is the matrix sparsification with maximum entropy, we observe its accuracy is still higher than the other two sparsifications. For example in the case of b = 8, the truncation based sparsification has maximum waveform error up to 0.03V (3% error when given input volatge swing is 1V), but the Shcur's windowing has 9X smaller error. We also find the heuristic windowing can achieve a acceptable error in all the window size settings.

We further present the waveform in Fig. 3 for the 128-bit bus example (with 8192 mutual inductances). It shows waveforms of the full PEEC, the heuristic windowed (HW) VPEC, the Schur's windowed (SW) VPEC, and geometrical-truncation windowed (TW) VPEC. We apply 1-V transient with rising time 10ps at first bit and observe the response at far-end of all other quiet bus. The size of the window (i.e. the band width b) in Fig. 3 is 16, and results similar 89.6% sparsification. The transient response shown in the figure is measured at far-end of 2nd bit. All the sparsified VPEC models achieve 30X speedup (9.7s vs. 280.7s) when compared to the PEEC model. Clearly, the transient response of TW method has non-negligible difference compared to the full PEEC model. On the other hand, the HW and SW methods are still comparable in term of the accuracy to the full PEEC model.

VI. Conclusions

To efficiently but yet accurately extract sparsified vector potential equivalent circuit (VPEC) model for inductive interconnects, we have developed two windowing methods to obtain a sparse approximated VPEC models. One is similar to windowing technique originally developed for the susceptance based method [4] and is called heuristic windowing in this paper. The other is based on the generalized Schur's algorithm and is called Schur's windowing. Both methods avoid inverting the full inductance matrix and have the faster extraction time and higher accuracy compared to the truncation-based windowing in [7] for large sized inductive interconnects. Furthermore, the Schur's windowing guarantees the symmetric positive definite property of the resulting circuit matrix without any heuristic selection as in the heuristic windowing, and achieves the best accuracy among all aforementioned windowing methods.

References

[1] A. E. Ruehli, "Equivalent circuits models for three dimensional multiconductor systems," *IEEE TMTT*, pp. 216–220, 1974.

[2] Z. He, M. Celik, and L. Pillegi, "SPIE: Sparse partial inductance extraction," in *DAC*, pp. 137–140, 1997.

[3] A. Devgan, H. Ji, and W. Dai, "How to efficiently capture on-chip inductance effects: introducing a new circuit element K," in *ICCAD*, pp. 150–155, 2000.

[4] M. Beattie and L. Pileggi, "Efficient inductance extraction via windowing," in *DATE*, pp. 430–436, 2001.

[5] T. Chen, C. Luk, and C. Chen, "Inductwise: Inductance-wise interconnect simulator and extractor," *ICCAD*, pp. 884–894, 2002.

[6] A. Pacelli, "A local circuit topology for inductive parasitics," in *ICCAD*, pp. 208–214, 2002.

[7] H. Yu and L. He, "Vector potential equivalent circuit based on PEEC inversion," in *DAC*, 2003.

[8] M. Kamon, M. Tsuk, and J. White, "FastHenry: a multipole-accelerated 3D inductance extraction program," *IEEE TMTT*, pp. 1750–1758, Sept. 1994.

[9] J. D. Jackson, *Classical Electrodynamics*. John Wiley and Sons, 1975.

[10] H. Dym and I. Cohberg, "Extensions of band matrices with band inverses," *Linear Algebra and its applications*, 1981.

[11] P. Dewilde, "New algebraic methods for modeling large-scale intergrated circuits," *International Journal of circuit Theory and Applications*, 1988.

[12] N. P. van der Meijs, "Space for substrate resistance modeling," in *Substrate Noise Coupling in Mixed Signal ASICs, G. Gielen and S. Donnay (ed.), Kluwer*, 2003.

[13] K. Narbos and J. White, "FastCap: A multipole accelerated 3D capacitance extraction program," *IEEE TCAD*, vol. 10, no. 11, pp. 1447–1459, 1991.